Journal of Applied Physics ARTICLE pubs.aip.org/aip/jap

New insights into diffusion–collection modeling of radiation-induced charge in semiconductor devices

Cite as: J. Appl. Phys. **134**, 175701 (2023); doi: 10.1063/5.0156698
Submitted: 2 May 2023 · Accepted: 12 October 2023 ·
Published Online: 1 November 2023

J. L. Autran[1,a)] and D. Munteanu[2]

AFFILIATIONS

[1]Aix-Marseille Université, CNRS, IM2NP (UMR 7334), Marseille, France and Université de Rennes, CNRS, IPR (UMR 6251), Rennes, France
[2]Aix-Marseille Université, CNRS, IM2NP (UMR 7334), Marseille, France

[a)]**Author to whom correspondence should be addressed:** jean-luc.autran@univ-rennes.fr

ABSTRACT

Charge diffusion from an ion track and its collection by a biased contact in a semiconductor domain is modeled and analyzed within the framework of the so-called diffusion–collection approach. We successively examine the case of charge diffusion from a point source and from a linear distribution, introducing and discussing the concept of collection velocity at the point where the collection current is evaluated. Analytical formulations of the collected charge, collection current, and collection velocity are developed. Implications for the calculation of the soft error rate in complementary metal-oxide-semiconductor circuits exposed to ionizing particles are derived. Finally, our model provides new insights into the correct definition of the charge collection velocity in collection–diffusion models.

I. INTRODUCTION

The passage of an ionizing particle through a semiconductor device results in energy transfer and the creation of electron–hole pairs along the particle track.[1,2] Carriers in excess are then transported by ambipolar diffusion throughout the volume of the semiconductor until they recombine or are collected and extracted, generally under the influence of an electric field developed by a biased contact or a reverse-biased p-n junction.[3] Modeling these different physical processes is essential to predict the transient electrical response of complementary metal-oxide-semiconductor (CMOS) devices and circuits subjected to ionizing particles and to evaluate their soft error rate (SER), i.e., the probability of an ionizing particle to cause a transient error in the circuit that affects its operation, without causing permanent damage.[2,4] Over the last 40 years, several modeling and numerical simulation studies have been carried out in the field of radiation-induced charge diffusion and collection in CMOS devices and circuits. Among these works are several pioneering contributions by Kirkpatrick,[5] Messenger,[6] Edmonds,[7] or Palau *et al.*,[8] followed in the last two decades by further contributions in this field,[9–19] which have benefited from increasingly efficient computing resources and simulation tools. Our analysis of these works has uncovered challenges in computing carrier collection current and assessing the circuit soft error rate. Starting from the fundamental equations of diffusion–collection, we, therefore, aimed to revisit established results that have been questioned as to their ability to explain the physical mechanisms involved in charge collection and how this process is controlled. More precisely, in this work, we model and analyze the diffusion of charge from an ion track and its collection by a contact in silicon. First, we reassess the case of charge diffusion from a point source and examine the methods for modeling the collected current and charge by a small contact at a particular distance from the source, while considering two diverse formalisms for the current: a pure diffusion current or a conduction current that incorporates a collection velocity. For the two approaches, we derive analytical expressions for the time dependence of both collected current and charge. In the second part, we revisit charge diffusion–collection from a linear distribution (emulating an ion track with constant linear energy deposition). We notice that previous solutions derived for the point source result in different representations of the collected charge depending on the chosen formalism for the current

(pure diffusion current or conduction current). Implications for the calculation of the SER of CMOS circuits exposed to ionizing particles are derived and discussed in the last part of this paper as well as the important issue of the collection velocity evaluation in diffusion–collection models. The series of analytical developments described below provide new insights into collection-diffusion models and the physical mechanisms involved, particularly in charge collection and the control of such a collection process. In addition, these models should enable a more accurate modeling of the SER of CMOS circuits, incorporating the essential physics of diffusion and collection of radiation-induced charge within the semiconductor.

II. CHARGE DIFFUSION AND COLLECTION FROM A POINT SOURCE

We first consider a point charge $Q = qn_0$ deposited at $t = 0$ in point M located in the bulk of a semiconductor domain. Despite this configuration implies an infinite homogeneous half-space, bounded by a planar surface, as represented in Fig. 1, in the following we neglect the reflective boundary condition on the silicon surface and consider the 3D simulation domain as an infinite medium. This point charge corresponds to a number n_0 of carriers-in-excess, for example, a number of electrons issued from a punctual energy transfer resulting in the creation of the same number of electron–hole pairs at $t = 0$ in M (the transport of holes will not be detailed in the following). Q is treated as a Dirac delta function of r, i.e., $Q(r) = qn_0(r)$. In the pure diffusion approach, the transport of excess carrier density n_e (m^{-3}) is governed by a 3D spherical diffusion law in the semiconductor domain,[5–7]

$$\frac{\partial n_e(r,t)}{\partial t} - \frac{n_e(r,t)}{\tau} = D\nabla^2 n_e(r,t), \tag{1}$$

where τ is the carrier lifetime and D is the ambipolar diffusion coefficient given by

$$D = 2D_nD_p/(D_n + D_p), \tag{2}$$

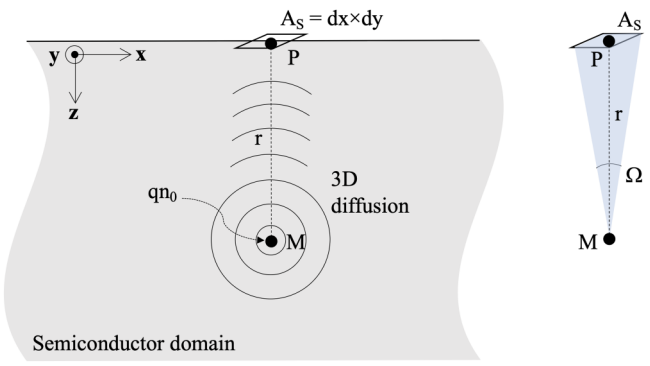

FIG. 1. Schematic illustration of diffusion from a point charge and the collection by a small contact of surface A_S.

with D_n and D_p being the diffusion coefficients for electrons and holes, respectively. The excess carrier density at time t and distance r originating from this point charge n_0 and solution to Eq. (1) can be written under the following form:[6]

$$n_e(r,t) = \frac{n_0}{(4\pi Dt)^{\frac{3}{2}}}\exp\left(-\frac{r^2}{4Dt} - \frac{t}{\tau}\right). \tag{3}$$

Neglecting carrier recombination in the following ($\tau \to +\infty$), which represents a strong simplification of the model but an imperative to maintain its analytical character, Eq. (3) can be used to calculate the charge collected in point P (see Fig. 1) by a small contact of surface A_S developing no electric field in the semiconductor. To do this, we have to evaluate the current density in point P and then integrate it on the contact surface and in time, from 0 to infinity. Two different formalisms can be used at this level to evaluate this quantity: the theory of diffusion or the general electrokinetic formulation of conduction.

A. Pure diffusion current

The expression of diffusion current density is

$$\vec{J}_{diff}(r,t) = qD\vec{\nabla}(n_e), \tag{4}$$

where the diffusion coefficient in this equation is the ambipolar diffusion because it corresponds to the considered carrier transport mechanism. Considering a small electrode centered in P (see Fig. 1) and the case where the diffusing carrier flux is perpendicular to the collecting surface, the diffusion current evaluated at the contact is

$$I_{diff}(r,t) = \iint_{A_S} J_{diff}(\vec{r},t)\cdot\vec{dS} \approx qA_SD\frac{\partial n_e(r,t)}{\partial r}, \tag{5}$$

where A_S is the surface of the electrode (assumed to be sufficiently "small" with respect to all other geometrical dimensions to avoid numerical integration in the current expression).

The time integration of Eq. (5) leads to the expression of the charge that diffuses to the electrode surface at P (which is then collected), originating from qn_0 at M. From Eqs. (3) and (5), we obtain

$$\left|I_{diff}(r,t)\right| = \frac{qA_Sn_0}{(4\pi D)^{\frac{3}{2}}}\times\frac{r}{2t^{\frac{5}{2}}}\times\exp\left(-\frac{r^2}{4Dt}\right) = qA_Sn_e(r,t)\times\frac{r}{2t}, \tag{6}$$

$$q_{col}^{diff}(r,t) = \int_0^t I_{diff}(r,t')\,dt' = \frac{qA_Sn_0}{2(\pi)^{\frac{3}{2}}r^2}\times\Gamma\left(\frac{3}{2},\frac{r^2}{4Dt}\right), \tag{7}$$

where $\Gamma(a,x)$ is the upper incomplete gamma function.[20] For ($t \to +\infty$), the gamma function term in Eq. (7) reduces to the quantity $\sqrt{\pi}/2$, and the maximum collected charge has the

following expression:

$$q_{col}^{diff}(r) = qn_0 \times \frac{A_S}{4\pi r^2}. \tag{8}$$

Another interesting quantity is the ratio $q_{col}^{diff}(r)/qn_0$ that corresponds to a collection efficiency for the collecting contact,

$$\eta_S^{diff} = \frac{q_{col}^{diff}(r)}{qn_0} = \frac{A_S}{4\pi r^2}. \tag{9}$$

Arranged under this form, the quantity $\Omega = A_S/4\pi r^2$ corresponds to the ratio of the solid angle of the collecting contact centered in point P and observed from point M to the solid angle for the entire space (see Fig. 1), as considered in Ref. 12. This collection efficiency, thus, appears to be proportional to the collector surface and inversely proportional to the square of the distance between the deposited charge and the collector.

At this level, we establish two interesting results for the times at which $n_e(r, t)$ and $I_{diff}(r, t)$ admit a maximum. From the time derivative of Eqs. (3) and (6), it is easy to show that

$$\left.\frac{\partial n_e(r,t)}{\partial t}\right|_{t=t_{max}^n} = 0 \Leftrightarrow t_{max}^n = \frac{r^2}{6D}, \tag{10}$$

$$\left.\frac{\partial I_{diff}(r,t)}{\partial t}\right|_{t=t_{max}^i} = 0 \Leftrightarrow t_{max}^i = \frac{r^2}{10D}. \tag{11}$$

This result is *a priori* counter-intuitive: the charge and the diffusion current do not pass through a maximum at the same time, contrary to what is assumed in Ref. 8, but the current reaches its maximum slightly before the charge. The maximum values for the charge and the current are as follows:

$$n_{e,max}(r) = n_e\left(r, t_{max}^n\right) = n_0\left(\frac{2}{3}\pi e r^2\right)^{-\frac{3}{2}}, \tag{12}$$

$$I_{diff,max}(r) = I_{diff}\left(r, t_{max}^i\right) = \left(\frac{5}{e}\right)^{\frac{5}{2}} \times \frac{qA_S n_0 D}{(2\pi)^{\frac{3}{2}} r^4}. \tag{13}$$

Figure 2 shows the time evolution of the carrier density and the diffusion current evaluated using Eqs. (3) and (6) for a distance $r = 1.5\,\mu$m from a point charge source $Q = qn_0$.

The curves highlight the time shift between the two transients: the current transient peak precedes the carrier density peak, with a peak position extracted at 0.163 ns against 0.272 ns for the density curve. This example also numerically illustrates that the time position and magnitude of the maximum of the two peaks verify the analytical expressions of Eqs. (10) to (13) that give $t_{max}^i = 0.1631$ ns, $t_{max}^n = 0.2718$ ns, $I_{diff,max} = 0.6231\,\mu$A, and $n_{e,max} = 3.308 \times 10^{16}$ cm^{-3}.

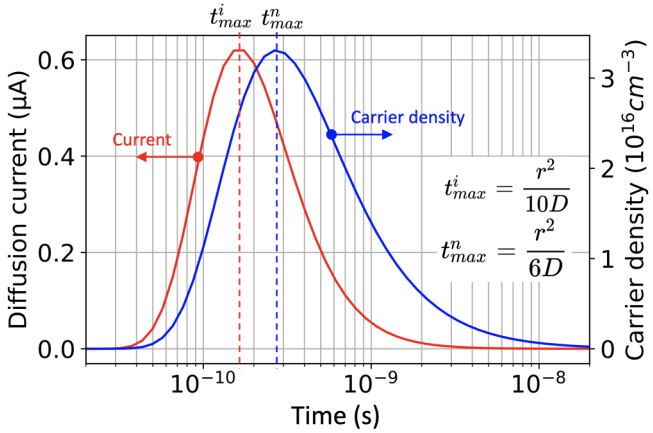

FIG. 2. Time evolution of the carrier density and the diffusion current evaluated from Eqs. (3) and (6), respectively, for a distance $r = 1.5\,\mu$m from a point charge source $Q = qn_0$. Simulation parameters are as follows: $n_0 = 1.52 \times 10^6$ electrons, $D = 13.78$ cm^2 s^{-1}, and $A_S = 0.0323\,\mu$m^2.

B. Conduction current

Instead of choosing the diffusion current formalism, one can consider the general electrokinetic equation for the current density carried by electrons of density n given by

$$\vec{J} = qn\vec{v}, \tag{14}$$

where v is the electron diffusion velocity. Using Eq. (3) for the carrier density n_e at point P (these carriers being transported by diffusion from source M to point P) and integrating Eq. (14) over the surface A_S give the collected current,[8]

$$I_{col}(r, t) = qA_S v_{col} n_e(r, t), \tag{15}$$

where the carrier diffusion velocity is denoted as v_{col} for "collection velocity" because it corresponds to the velocity at which the carriers are collected by crossing the collecting surface of the contact, in the absence of an electric field, and transported only by the diffusion process.

The equality of current densities expressed from Eqs. (4) and (14) at the point of collection leads to a general expression of this collection velocity under the following form:

$$qD\vec{\nabla}(n_e) = qn_e\vec{v}_{col} \Rightarrow \vec{v}_{col} = D\frac{\vec{\nabla}(n_e)}{n_e}. \tag{16}$$

The direct comparison of Eqs. (6) and (15), which must correspond to the same current, forces the term v_{col} to take the following expression:

$$(6) = (15) \Rightarrow v_{col} = \frac{r}{2t}. \tag{17}$$

This quantity has the physical dimension of a velocity that is position and time dependent. The expression of $v_{col}(r, t)$ given by Eq. (17) ensures that the conduction current equals the diffusion

current at the position where the two quantities are evaluated. Of course, it is evident that using the conduction current given by Eq. (15) with the above collection velocity leads to the same collected charge as that given by Eqs. (7) and (8). We will come back in detail to this concept of collection velocity in Sec. V.

C. Case of lateral diffusion

The case of lateral diffusion should be examined since it is different from the previous case (see Fig. 1) where the carrier flux is perpendicular to the collecting electrode. We first examine the case of the ideal planar collecting contact, as represented in Fig. 3(a) and previously considered. The solid angle of the contact viewed from point M is, in this case, equal to

$$\Omega = \frac{A_S \times \cos(\alpha)}{4\pi r^2} = \frac{A_S \ell}{4\pi r^3}. \tag{18}$$

Considering Eq. (18), Eqs. (7) and (8) must then be rewritten under the following form:

$$q_{col}^{diff}(r, \ell, t) = \frac{qA_S n_0 \ell}{2(\pi)^{\frac{3}{2}} r^3} \times \Gamma\left(\frac{3}{2}, \frac{r^2}{4Dt}\right), \tag{19}$$

$$q_{col}^{diff}(r, \ell) = qn_0 \times \frac{A_S \ell}{4\pi r^3}. \tag{20}$$

These expressions predict a collected charge equal to zero for $\ell = 0$. In other words, as the point source moves closer to the surface, the collected charge reduces until it reaches zero for a source situated on the semiconductor's surface. However, this scenario does not correspond to reality, as collector contacts (also known as sensitive circuit nodes) in CMOS technologies are never planar contacts with no physical thickness, but rather ohmic contacts (N^+N or P^+P junctions with low resistance and non-rectifying properties) or reverse-biased junctions (N^+P or P^+N). Such devices have a physical extension in depth that corresponds to the space charge region of the junction. Therefore, a "real" collector contact, as schematically represented in Fig. 3(b), is characterized by two surfaces:

- an horizontal surface (A_S) that represents the contact area at the "layout" level and that also corresponds to the lower face of the space charge region in the semiconductor; and
- a vertical surface (A_L) that corresponds to the side surface of the space charge region in the semiconductor.

The diffusion current is, thus, obtained by integrating the current density on the whole collector surface inside the semiconductor (i.e., on the lateral + lower surfaces),

$$I_{diff}(r, l, t) = \iint_{A_S+A_L} J_{diff}(\vec{r}, t) \cdot \vec{dS} \approx qD \frac{\partial n_e(r, \ell, t)}{\partial r} \times A_C(M), \tag{21}$$

where $A_C(M)$ is the effective collection surface viewed from point M, i.e., the collector surface in direct view from the point source. The approximation made in Eq. (21) requires that the dimensions of the collector are small compared to the source-to-collector distance. Equations (7) and (8) and all derived equations still apply in the case of lateral diffusion with A_S formally replaced by the quantity $A_C(M)$. From these equations, the collected charge is never equal to zero when M is located at the semiconductor surface ($\ell = 0$). Because $A_C(M)$ is difficult to evaluate for a realistic junction geometry from analytical calculations, in the following we make the assumption that $A_C(M) \approx A_S$ whatever the point M in the semiconductor domain (sufficiently far enough from the contact), which is an acceptable approximation in the case of "box" geometries of the collector.

III. CHARGE DIFFUSION AND COLLECTION FROM A LINE SOURCE

From the previous results in the effective collection surface approximation, the total collected charge at the collecting contact resulting from the contribution of a particle track can be evaluated from Eq. (8), considering a track as an ensemble of point charges uniformly distributed along a straight segment. We consider the simplified case, as shown in Fig. 4, where a ionizing particle perpendicularly arrives to the semiconductor surface. The particle is assumed to lose energy ΔE along the segment [IF] of length L. Considering an energy of electron–hole pair creation equal to $E_{e,h}$

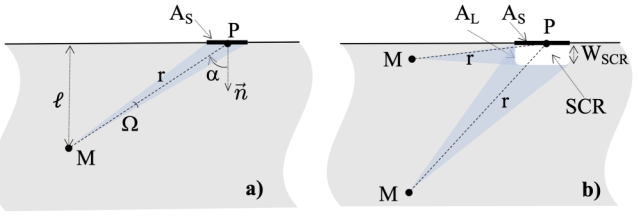

FIG. 3. Schematic illustrations of collecting contacts: (a) An ideal planar contact of surface A_S and (b) a "real" contact in CMOS circuits consisting of a reverse biased junction with a layout surface A_S and a lateral surface A_L due to depth extension (W_{SCR}) of the space charge region (SCR).

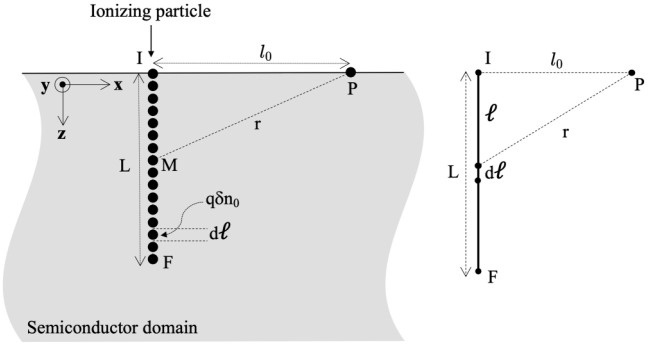

FIG. 4. Schematic illustration of the case of a particle track considered as an ensemble of point charges $q\delta n_0$ uniformly distributed along a straight segment of length L.

for the target semiconductor material, the particle creates a total of $N = \Delta E/E_{e,h}$ pairs.

For simplicity, we suppose a constant linear energy transfer (LET) value: this charge is, thus, uniformly deposited along the ion track. In this case, each elementary segment of length $d\ell$ carries an elementary charge δn_0 supposed punctual,

$$\delta n_0 = \frac{N}{L} \times d\ell = \frac{\Delta E}{E_{e,h} L} \times d\ell, \tag{22}$$

where ℓ and $d\ell$ are defined in Fig. 4. The integration of Eq. (8) along the particle track using Eq. (22) gives the total collected charge at the collecting contact,

$$Q_{col}^{diff} = \frac{qA_S N}{4\pi L} \int_0^L \frac{d\ell}{l_0^2 + \ell^2}. \tag{23}$$

We obtain

$$Q_{col}^{diff} = Q_0^{diff} \times arctan\left(\frac{L}{l_0}\right), \tag{24}$$

with

$$Q_0^{diff} = \frac{qA_S N}{4\pi L l_0}. \tag{25}$$

Finally, and similarly to Eq. (9), we can define a collection efficiency for the collection from a line source. From Eqs. (24) and (25), we obtain

$$\eta_S^{diff} = \frac{Q_{col}^{diff}}{qN} = \frac{A_S}{4\pi L l_0} \times arctan\left(\frac{L}{l_0}\right). \tag{26}$$

Equation (26) reduces to Eq. (9) with $r = l_0$ when $L/l_0 \to 0$.

IV. IMPLICATIONS FOR THE EVALUATION OF THE SOFT ERROR RATE OF CMOS CIRCUITS

Equation (24) with the prefactor term defined in Eq. (25) shows that the collected charge at the level of a small collecting contact is a function of l_0, the distance between the track and the contact, as defined in Fig. 4. Solving this equation allows us to define a critical distance $l_0 = l_{crit}$ from the contact below which any ionizing particle (characterized by a certain N/L value) will produce a collected charge of at least a given amount called the critical charge Q_{crit}. The critical charge is a key factor for measuring the circuit's vulnerability to radiation. It specifies the amount of charge necessary to trigger a transition from a logical low to a logical high or vice versa at a sensitive node of the circuit. The concepts of critical distance and critical charge are illustrated in Fig. 5. The product of the disk surface of radius l_{crit} by the particle flux directly gives the soft error rate (*SER*), i.e., the rate at which errors occur at the level of the sensitive node (defined by the collecting surface A_S in P) of an electronic system or device,

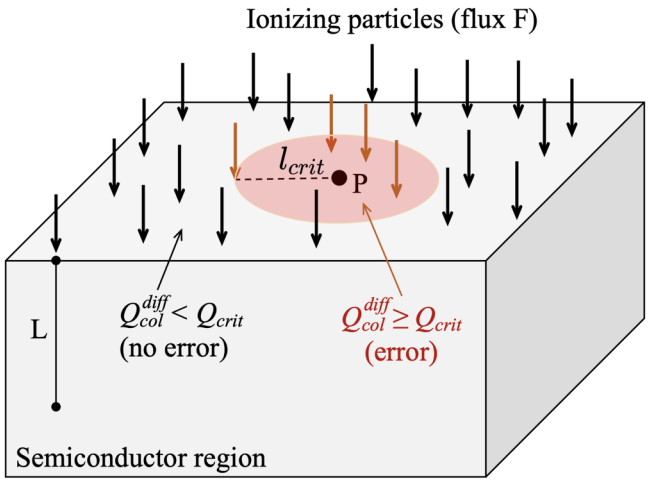

FIG. 5. Illustration of the concepts of critical distance l_{crit} and critical charge Q_{crit}. Any particle (characterized by the ratio N/L) that impacts the disk centered in P and of radius l_{crit} will result in a collected charge above Q_{crit} and then inducing a soft error.

$$SER = \pi l_{crit}^2 F, \tag{27}$$

where F is the particle flux ($m^{-2}\,s^{-1}$).

This *SER* is typically expressed in Failures-In-Time (FITs), which is a measure of the number of failures that can be expected in one billion device hours of operation.[2] For memory devices, the *SER* is given in FIT/Mbit, i.e., in FIT for 1024^2 memory cells. We detail in the following the derivation of l_{crit} and *SER* from the previous development used to evaluate the collected charge. As explained above, to determine l_{crit}, we have to solve Eqs. (24) and (25) for $Q_{col}^{diff} = Q_{crit}$ and $l_0 = l_{crit}$ as follows:

$$Q_{crit} = \frac{qA_S N}{4\pi L l_{crit}} \times arctan\left(\frac{L}{l_{crit}}\right). \tag{28}$$

Unfortunately, l_{crit} cannot be analytically determined from Eq. (28) because this equation is transcendental. Indeed, the term l_{crit} appears two times in the equation, both in the pre-factor and in the *arctan* argument, and only a numerical solving can be envisaged to determine l_{crit}. To remain analytical, we propose in the following to replace in Eq. (28) the *arctan* function by the well-known approximation:

$$arctan(x) \approx \frac{\pi}{2} \times \frac{x}{1 + |x|}. \tag{29}$$

Figure 6 shows the comparison of the *arctan* function and its approximation, evidencing a very good agreement over all the real axis. Introducing Eq. (29) in Eq. (24) in place of the *arctan* term

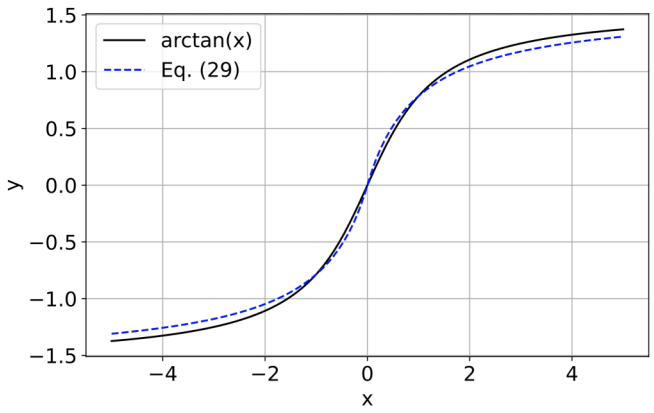

FIG. 6. Comparison of the *arctan*(*x*) function and its approximation defined in Eq. (29).

and rearranging the equation, we obtain

$$Q_{col}^{diff} = \frac{qA_SN}{4\pi l_0 L} \times \frac{\pi}{2} \times \frac{L/l_0}{1+L/l_0} = \frac{qA_SN}{8L^2} \times \frac{(L/l_0)^2}{1+L/l_0}. \quad (30)$$

Let $x = L/l_{crit}$, and $Q_{col}^{diff} = Q_{crit}$ can be rewritten under the form of a polynomial of degree two in x,

$$x^2 - Bx - B = 0, \quad (31)$$

with

$$B = \frac{8L^2 Q_{crit}}{qA_SN}. \quad (32)$$

The positive root of Eq. (31) directly gives l_{crit},

$$l_{crit} = \frac{2L}{B + \sqrt{B^2+4B}}. \quad (33)$$

The soft error rate is then expressed by

$$SER = \pi l_{crit}^2 F = \frac{4\pi L^2 F}{\left(B + \sqrt{B^2+4B}\right)^2}. \quad (34)$$

This *SER* vs Q_{crit} will be compared to other SER expressions and values in Sec. V.

V. LINK WITH OTHER DIFFUSION-COLLECTION FORMALISMS BASED ON THE COLLECTION VELOCITY

A. Time-independent collection velocity

In many studies carried out under the diffusion-collection framework, the expression of the collected current includes a collection velocity that remains constant over time.[8–16,18,19] The consequence of this approximation in the present developments is to remove this term from the time integration of the current, which leads to a different expression for the collected charge, called $q_{col}(r)$, diffusing from a point source,[19]

$$q_{col}(r) = qn_0 \times \frac{A_S v_{col}}{4\pi D r}. \quad (35)$$

The direct comparison of this expression with Eq. (8), which must correspond to the same quantity, forces the term v_{col} to be equal in this case to

$$(8) = (35) \Rightarrow v_{col} = \frac{D}{r}. \quad (36)$$

In such an approximation, v_{col} appears to be only position-dependent. Because this expression is obtained by comparing two expressions of the collected charge, which are the results of the current integration over time, Eq. (36) must not be used in Eq. (15) to express the conduction current, since it would no longer be in balance with the diffusion current. In other words, this approximation of v_{col} only makes sense at the level of the expression of the collected charge, not at the level of the current.

Equation (36) can be used to calculate an average value of the collection velocity for a particle track defined in Fig. 4 (see Appendix). With such a constant value $< v_{col} >$ and similarly to what has been done in Sec. III, the integration of Eq. (35) along the particle track gives a different expression of the total collected charge Q_{col} at the collecting contact,

$$Q_{col} = \frac{qA_SN < v_{col} >}{4\pi DL} \int_0^L \frac{d\ell}{\sqrt{l_0^2 + \ell^2}}. \quad (37)$$

We obtain

$$Q_{col} = Q_0 \times arsinh\left(\frac{L}{l_0}\right), \quad (38)$$

with

$$Q_0 = \frac{qA_SN < v_{col} >}{4\pi DL}, \quad (39)$$

where *arsinh*(*x*) is the inverse hyperbolic sine, defined over the whole real line and given by

$$arsinh(x) = ln\left(x + \sqrt{x^2+1}\right). \quad (40)$$

Finally and similarly to Eq. (26), we can define a collection efficiency,

$$\eta_S = \frac{Q_{col}}{qN} = \frac{A_S < v_{col} >}{4\pi DL} \times arsinh\left(\frac{L}{l_0}\right). \quad (41)$$

Equation (38) with prefactor defined by Eq. (39) represents *a priori* a severe approximation of Eqs. (24) and (25) because the collection velocity v_{col} [which is position-dependent, as established in

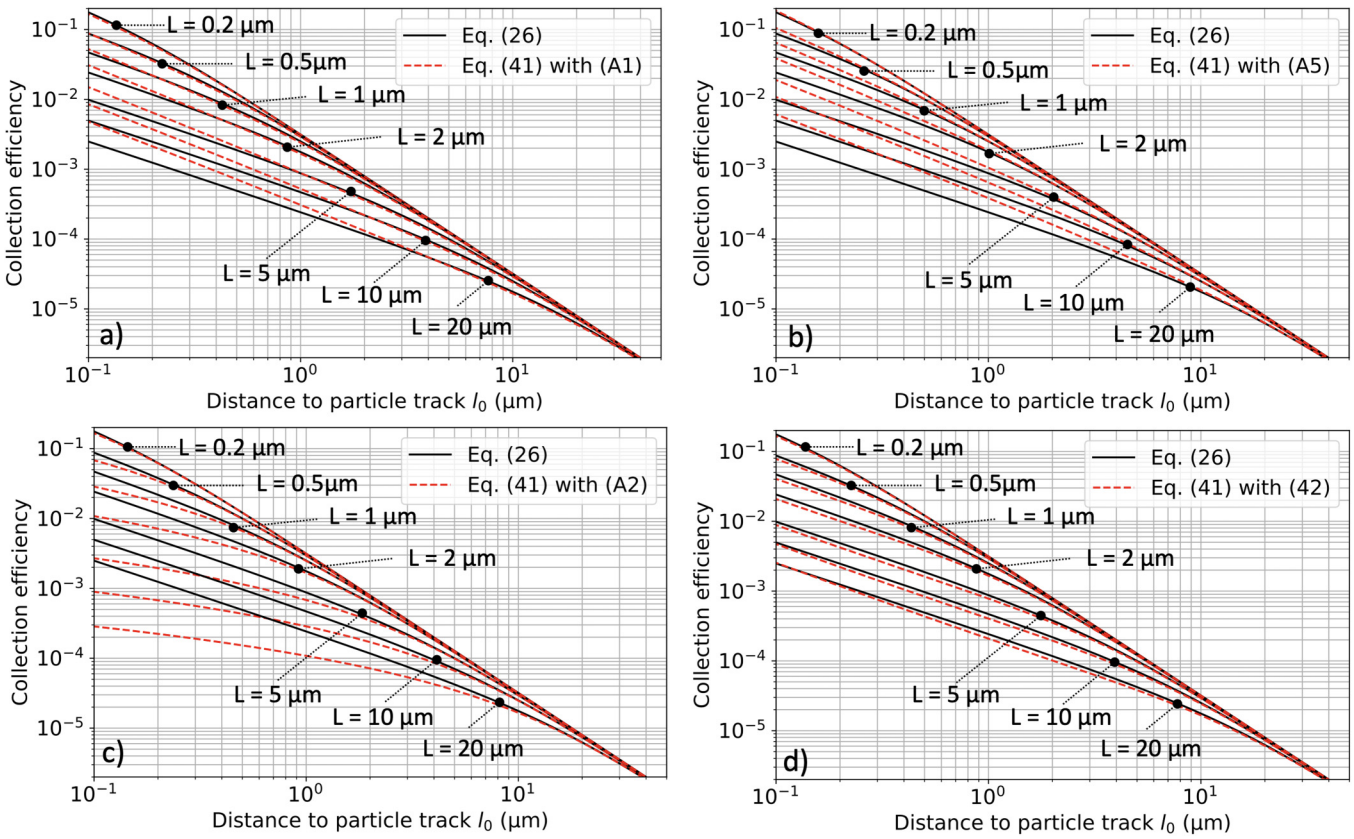

FIG. 7. Comparison of the collection efficiency given by Eq. (26) exactly derived from the diffusion current with collection efficiencies computed from Eq. (41) considering the average collection velocities given by (a) Eq. (A1); (b) Eq. (A5); (c) Eq. (A2); and (d) Eq. (42).

Eq. (36)] is now becoming a constant. This approximation is numerically evaluated in Figs. 7(a)–7(c). This figure compares the collection efficiency computed from Eq. (41) considering the different average collection velocities defined in the Appendix with the collection efficiency defined by Eq. (26) exactly derived from the diffusion current. Results of Figs. 7(a)–7(c) show that the agreement between the two efficiencies is reasonable for the different $< v_{col} >$ values. The smaller the range of the particle and the greater the distance between the particle strike and the contact, the better the agreement. Results are more satisfactory with $< v_{col} >$ given by Eq. (A1) or Eq. (A5) than with Eq. (A2). The reason is that Eqs. (A1) and (A5) give more weight to the contribution of the particle track that is closest to the collector, in contrast to a uniform average over the entire track.

As a result, average velocities given by Eqs. (A1) or (A5) lead to a slight overestimation of the collection efficiency for $l_0 < 1\,\mu$m, whereas Eq. (A2) clearly underestimates the collection efficiency for $L > 2\,\mu$m and for $l_0 < 2\,\mu$m. These numerical results suggest that if an average velocity $< v_{col,4} >$ is taken as the average of the velocities given by Eqs. (A1) or (A2), the observed underestimation and overestimation should be compensated, and the agreement of the results could then be better. We, thus, introduce

$$< v_{col,4} >= \frac{1}{4}\left(\frac{D}{l_0} + \frac{D}{\sqrt{l_0^2 + L^2}}\right) + \frac{D}{2L} arsinh\left(\frac{L}{l_0}\right). \quad (42)$$

This result is fully confirmed in Fig. 7(d) with a very nice agreement observed between the two collection efficiencies for all values of l_0 and L ranging from 0.1 to 40 μm. Figure 7(d) shows that the deliberate choice to remove the collection velocity from the integral term in Eq. (37), therefore, appears to be numerically justified as long as a correct average velocity of the carriers diffusing from the track is used.

In practice, the error made by considering Eqs. (38) and (39) instead of Eqs. (24) and (25) should be limited by the different $< v_{col} >$ expressions if the track length L is limited to a few micrometers or, for longer ranges, if the track-to-contact distance l_0 is typically greater than a few micrometers.

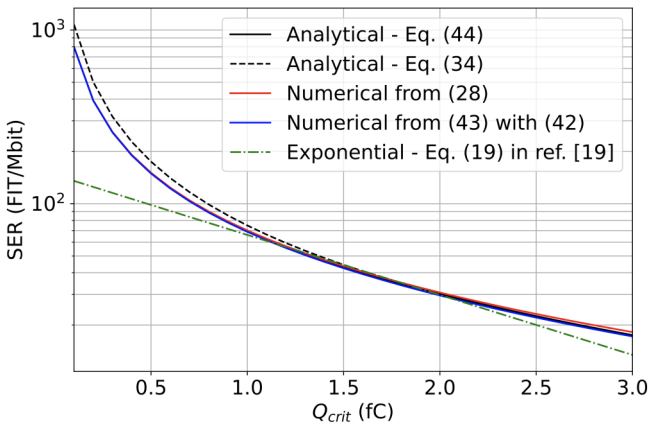

FIG. 8. *SER* vs Q_{crit} computed from analytical Eqs. (34) and (44), from the numerical solving of Eq. (28), of Eq. (43) considering collection velocity given by Eq. (42) and from an exponential approximation [Eq. (19) in Ref. 19] close to the empirical expression proposed by Hazucha and Svensson.[21] Simulation parameters are as follows: $A_S = 0.25\,\mu m^2$, $L = 2\,\mu m$, $N = 1.38 \times 10^6$, $D = 61\,cm^2\,s^{-1}$, $F = 10^{-3}\,cm^{-2}\,h^{-1}$, and $v_{col} = 3.5 \times 10^5\,cm\,s^{-1}$ for Eq. (19) in Ref. 19.

As in Sec. IV, to obtain the SER, one has to solve Eq. (38) with $Q_{col} = Q_{crit}$ and $l_0 = l_{crit}$, i.e.,

$$Q_{crit} = Q_0 \times arsinh\left(\frac{L}{l_{crit}}\right). \tag{43}$$

The main advantage of considering a constant collection velocity is that Eq. (43) can be solved analytically in two interesting cases: (i) $< v_{col} >$ is reduced to a single numerical value or (ii) $< v_{col} > = < v_{col,2} >$ given in the Appendix [Eq. (A2)]. In the first case, the *SER* is identical to the value reported in Ref. 19. In the second case, due to the presence of the term $arcsinh(L/l_0)$ in the expression of $< v_{col} >$, this term can be factorized, and the resulting *SER* is equal to

$$SER = \pi L^2 F \times \left[\sinh\left(\sqrt{\frac{Q_{crit}}{Q_0}}\right)\right]^{-2}. \tag{44}$$

In other cases, i.e., for the numerical solving of Eq. (28) or Eq. (43) with the most accurate $< v_{col} >$ given by Eq. (42), a simple numerical solving of the equation $Q_{col}(l_{crit}) = Q_{crit}$ can be performed using the dichotomy or Newton–Raphson methods, for example.[22]

Figure 8 compares the *SER* vs Q_{crit} curves for these different equations and resolution methods, considering the analytical *SER* expressions given by Eqs. (34) and (44), the numerical solving of Eq. (28) and Eq. (43) with the collection velocity given by Eq. (42), and finally the exponential expression, close to the empirical expression proposed by Hazucha and Svensson,[21] proposed in Ref. 19 [Eq. 19 in the reference]. The simulation parameters are reported in the caption of Fig. 8. The different expressions obtained in the present work exhibit a non-exponential dependence of the *SER* on the critical charge. In particular, there is a large increase in the *SER* at low Q_{crit} values. However, as shown in Fig. 8, over a significant interval of Q_{crit} values (here between 1 and 2.2 fC), all $SER(Q_{crit})$ curves exhibit a quasi-exponential behavior. More generally, for relatively limited intervals of Q_{crit}, these distributions can be approximated by an exponential law. This is generally the case for experimental data reported in the literature, where the critical charge ranges are limited for technological reasons. This could explain why such non-exponential variations are not observed and why the exponential dependence of the *SER* is systematically taken into account in its modeling. Although non-exponential, the expressions of the *SER* proposed in the framework of this study, in particular, Eqs. (27) and (28) and their approximation [Eq. (34)], remain fully compatible with the observed variations in the *SER* over limited intervals of variation in the critical charge.

B. About the nature and interpretation of collection velocity

In addition to the previous point, it seems that there has long been confusion in the literature about the nature of the collection velocity introduced in diffusion–collection models. For example, in Ref. 8 but also in Refs. 9–19 (including certain of our own past work), the authors consider that the collection velocity corresponds to *"the average velocity of the carriers in the space charge region of the drain junction."*[8] As discussed below, this definition is not correct for the velocity used in Eq. (14), but it has had almost no impact on the published results because, until now, this velocity has not been calculated but rather extracted as a fitting parameter from numerical technology computer-aided design (TCAD) simulations. These simulations solve the Poisson and continuity equations in a self-consistent manner, usually within the framework of a drift-diffusion transport model. In this sense, they properly take into account the diffusion of carriers during their transport in the semiconductor, from deposition to the collection points. As a result, the extracted velocity value is correct and the resulting calculated current corresponds to a pure diffusion current.

Figure 9 schematically represents the case of charge diffusion from a point source and its collection by a reverse-biased N^+P junction, representative of a sensitive drain in a CMOS circuit. We focus on the particular situation at point P, located at the border of the space charge region created by the junction. On one hand, the carrier flux coming from M gives in P, on the bulk semiconductor side, a current density of pure diffusion expressed by Eq. (4) or by Eq. (14) with Eq. (42). On the other hand, when these carriers cross the boundary of the SCR, they are driven by the electric field F of the junction and give rise to a drift current density. This transformation of the nature of the current should not hide the fact that the continuity of the current densities must be respected: the diffusion current density at the boundary between the neutral region of the substrate (i.e., the diffusion domain) and the extremity of the junction SCR is equal to the carrier drift current density inside the SCR (i.e., the drift domain). The consequence for the charge collection mechanism of a reverse-biased junction is important: carriers arriving at the boundary of the SCR and being literally sucked in

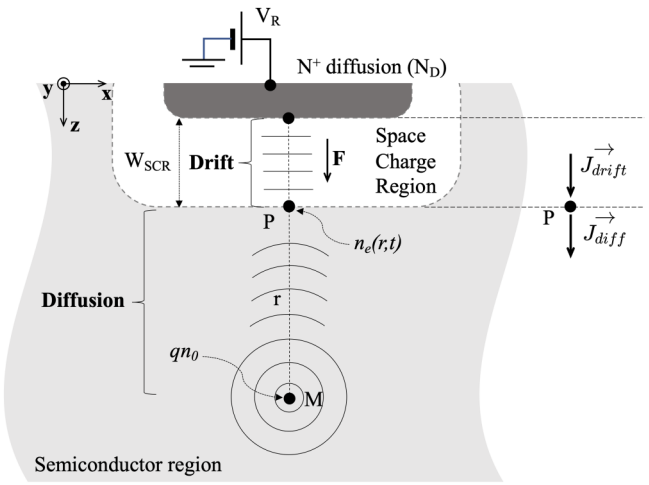

FIG. 9. Schematic illustration of diffusion from a point charge and the collection by a reverse-biased N^+P junction.

by the electric field of the junction are those that contribute to the collected charge. If carrier recombination is neglected, the intensity of the electric field inside the SCR, therefore, does not matter: for the carriers arriving at the edge of the SCR, their subsequent transport into the SCR does not change the amount of collected carriers. This quantity depends only on the diffusion current density evaluated at the limit of the SCR and integrated on the surface separating it from the neutral zone of the semiconductor. The reverse bias (V_R) of the junction has only one main effect in charge collection: it controls the depth of the SCR and, thus, modulates the distance between the carrier source and the SCR (distance between points M and P in Fig. 9). This modulation has only a limited effect on the collection of the charges deposited in the vicinity of the collector contact, i.e., for short l_0 distances. Taking the example of an N^+P junction with respective doping levels of 3×10^{20} and $10^{18}\,\mathrm{cm}^{-3}$ (typical values for a deca-nanometer CMOS bulk technology), the extension of the SCR goes from 45 to 65 nm as the voltage V_R varies from 0.5 to 2 V. Modulating the depth of the SCR by no more than 20 nm will have an extremely limited effect on the charge collection efficiency of the junction.

VI. CONCLUSION

Despite a consequent amount of modeling and simulation works in the field of diffusion–collection of radiation-induced charges in semiconductor devices, some previous works have admitted questionable points for the understanding of the physical mechanisms involved, in particular, in the collection of charges and how such a collection process is controlled. This work has precisely revisited, from the basic equations of diffusion–collection, some results considered as established in the literature. Thus, we have reexamined the case of charge diffusion from a point source and from a linear distribution and determined analytical formulations for the collected charge from two different formalisms: the theory of diffusion and the general electrokinetic formulation of the conduction. We have shown that for a charge diffusing from a point source and being collected by a remote contact, the collected charge and current do not pass through a maximum at the same time, contrary to what it is widely assumed in the literature: the diffusion current reaches its maximum slightly before the charge. In the case of the conduction current formalism, we have reexamined the concept of collection velocity at the point where the collection current is evaluated. The implications for the calculation of the soft error rate in CMOS circuits exposed to ionizing particles have been explored. Finally, we have shown that in the diffusion–collection approach, the key quantity to evaluate is clearly the diffusion current density at the limit of the SCR of the collector contact. This quantity does not depend on the electric field inside the SCR but only on the distance from the carrier source (initial charge deposition) and on the parameters D and v_{col} that characterize the carrier dynamics in the neutral zone of the semiconductor. The collection velocity included in the expression of the collected current and charge does not depend on the internal parameters of the collector contact; it is a parameter that does not go beyond the exclusive framework of the carrier diffusion mechanism.

AUTHOR DECLARATIONS

Conflict of Interest

The authors have no conflicts to disclose.

Author Contributions

All authors contributed equally to this work.

J. L. Autran: Conceptualization (equal); Formal analysis (equal); Investigation (equal); Methodology (equal); Writing – original draft (equal); Writing – review & editing (equal). **D. Munteanu:** Conceptualization (equal); Formal analysis (equal); Investigation (equal); Methodology (equal); Writing – original draft (equal); Writing – review & editing (equal).

DATA AVAILABILITY

The data that support the findings of this study are available from the corresponding author upon reasonable request.

APPENDIX: DETERMINATION OF THE AVERAGE COLLECTION VELOCITY FOR A PARTICLE TRACK

From Eq. (35), different average values for an extended source, i.e., a particle track of length L located at the distance l_0 from the collecting contact (see Fig. 4), can be easily derived.

A first way is to roughly calculate the average value from the values evaluated at the two extremities of the track segment, i.e.,

$$< v_{col,1} > = \frac{1}{2}\left(\frac{D}{l_0} + \frac{D}{\sqrt{l_0^2 + L^2}}\right). \quad \text{(A1)}$$

A second way to evaluate v_{col} is to calculate its average value this time along the whole track segment, i.e.,

$$< v_{col,2} >= \frac{1}{L}\int_0^L \frac{D}{r}\, d\ell = \frac{D}{L}\int_0^L \frac{d\ell}{\sqrt{l_0^2+\ell^2}} = \frac{D}{L} arsinh\left(\frac{L}{l_0}\right). \quad \text{(A2)}$$

Finally, a third way to evaluate v_{col} is to weigh each segment $d\ell$ by the quantity $f(r) = 1/r^2$ to take into account the weighed contribution of the segment to the total collected charge,

$$< v_{col,3} >= \frac{1}{K}\int_0^L \frac{D}{r} f(r)\, d\ell = \frac{D}{K}\int_0^L \frac{d\ell}{(l_0^2+\ell^2)^{3/2}} = \frac{DL}{Kl_0^2\sqrt{l_0^2+L^2}}, \quad \text{(A3)}$$

with the normalization constant K given by

$$f(r) = \frac{1}{r^2} \Rightarrow \int_0^L f(r) d\ell = K = \frac{1}{l_0} arctan\left(\frac{L}{l_0}\right) \quad \text{(A4)}$$

that finally gives

$$< v_{col,3} >= \frac{DL}{l_0\sqrt{l_0^2+L^2}} \times \left[arctan\left(\frac{L}{l_0}\right)\right]^{-1}. \quad \text{(A5)}$$

REFERENCES

[1]C. Leroy and P. G. Rancoita, *Principes of Radiation Interaction Matter and Detection* (World Scientific Publishing Co. Pte. Ltd., 2004).
[2]J. L. Autran and D. Munteanu, *Soft Errors: From Particles to Physics* (CRC Press, 2015).
[3]M. Murat, A. Akkerman, and J. Barak, "Electron and ion tracks in silicon: Spatial and temporal evolution," IEEE Trans. Nucl. Sci. **55**, 3046–3054 (2008).
[4]D. Munteanu and J.-L. Autran, "Modeling and simulation of single-event effects in digital devices and ICs," IEEE Trans. Nucl. Sci. **55**, 1854–1878 (2008).
[5]S. Kirkpatrick, "Modeling diffusion and collection of charge from ionizing radiation in silicon devices," IEEE Trans. Electron Devices **26**, 1742–1753 (1979).
[6]G. C. Messenger, "Collection of charge on junction nodes from ion tracks," IEEE Trans. Nucl. Sci. **29**, 2024–2031 (1982).
[7]L. Edmonds, "Charged collected by diffusion from an ion track under mixed boundary conditions," IEEE Trans. Nucl. Sci. **38**, 834–837 (1991).
[8]J. M. Palau, G. Hubert, K. Coulie, B. Sagnes, M.-C. Calvet, and S. Fourtine, "Device simulation study of the seu sensitivity of srams to internal ion tracks generated by nuclear reactions," IEEE Trans. Nucl. Sci. **48**, 225–231 (2001).
[9]J.-M. Palau, R. Wrobel, K. Castellani-Coulie, M.-C. Calvet, P. Dodd, and F. Sexton, "Monte Carlo exploration of neutron-induced SEU-sensitive volumes in SRAMs," IEEE Trans. Nucl. Sci. **49**, 3075–3081 (2002).
[10]D. Lambert, J. Baggio, V. Ferlet-Cavrois, O. Flament, F. Saigne, B. Sagnes, N. Buard, and T. Carriere, "Neutron-induced SEU in bulk srams in terrestrial environment: Simulations and experiments," IEEE Trans. Nucl. Sci. **51**, 3435–3441 (2004).
[11]T. Merelle, H. Chabane, J.-M. Palau, K. Castellani-Coulie, F. Wrobel, F. Saigne, B. Sagnes, J. Boch, J. Vaille, G. Gasiot, P. Roche, M.-C. Palau, and T. Carriere, "Criterion for SEU occurrence in SRAM deduced from circuit and device simulations in case of neutron-induced SER," IEEE Trans. Nucl. Sci. **52**, 1148–1155 (2005).
[12]F. Wrobel, G. Hubert, and P. Iacconi, "A semi-empirical approach for heavy ion SEU cross section calculations," IEEE Trans. Nucl. Sci. **53**, 3271–3276 (2006).
[13]V. Correas, F. Saigne, B. Sagnes, J. Boch, G. Gasiot, D. Giot, and P. Roche, "Innovative simulations of heavy ion cross sections in 130 nm CMOS SRAM," IEEE Trans. Nucl. Sci. **54**, 2413–2418 (2007).
[14]V. Correas, F. Saigne, B. Sagnes, J. Boch, G. Gasiot, D. Giot, and P. Roche, "Simulation tool for the prediction of heavy ion cross section of innovative 130-nm SRAMS," IEEE Trans. Nucl. Sci. **55**, 2036–2041 (2008).
[15]L. Artola, G. Hubert, S. Duzellier, and F. Bezerra, "Collected charge analysis for a new transient model by tcad simulation in 90 nm technology," IEEE Trans. Nucl. Sci. **57**, 1869–1875 (2010).
[16]S. Uznanski, G. Gasiot, P. Roche, C. Tavernier, and J.-L. Autran, "Single event upset and multiple cell upset modeling in commercial bulk 65-nm CMOS SRAMS and flip-flops," IEEE Trans. Nucl. Sci. **57**, 1876–1883 (2010).
[17]L. Artola, G. Hubert, K. M. Warren, M. Gaillardin, R. D. Schrimpf, R. A. Reed, R. A. Weller, J. R. Ahlbin, P. Paillet, M. Raine, S. Girard, S. Duzellier, L. W. Massengill, and F. Bezerra, "SEU prediction from set modeling using multi-node collection in bulk transistors and SRAMS down to the 65 nm technology node," IEEE Trans. Nucl. Sci. **58**, 1338–1346 (2011).
[18]S. Martinie, J.-L. Autran, S. Sauze, D. Munteanu, S. Uznanski, P. Roche, and G. Gasiot, "Underground experiment and modeling of alpha emitters induced soft-error rate in CMOS 65 nm SRAM," IEEE Trans. Nucl. Sci. **59**, 1048–1053 (2012).
[19]J.-L. Autran and D. Munteanu, "Physics-based analytical formulation of the soft error rate in CMOS circuits," IEEE Trans. Nucl. Sci. **70**, 782–791 (2023).
[20]R. B. Paris, *Incomplete Gamma and Related Functions, Nist Handbook of Mathematical Functions* (Cambridge University Press, 2010), Chap. 8.
[21]P. Hazucha and C. Svensson, "Impact of CMOS technology scaling on the atmospheric neutron soft error rate," IEEE Trans. Nucl. Sci. **47**, 2586–2594 (2000).
[22]W. H. Press, S. A. Teukolsky, W. T. Vetterling, B. P. Flannery, and M. Metcalf, *Numerical Recipes in C: The Art of Scientific Computing*, 2nd ed. (Cambridge University Press, 1992), Chap. 9.